12th International Conference on Advances in Steel-Concrete Composite Structures (ASCCS 2018)
Universitat Politècnica de València, València, Spain, June 27-29, 2018
Doi: http://dx.doi.org/10.4995/ASCCS2018.2018.6993

Behaviour and Design of Composite Steel and Precast Concrete Transom for Railway Bridges Application

O. Mirza[a]*, A. Talos[a], M. Hennessy[a] and B. Kirkland[a]

[a]School of Computing, Engineering and Mathematics, Western Sydney University, Australia
*corresponding author, e-mail address: o.mirza@westernsydney.edu.au

Abstract

Currently most railway bridges in Australia require the replacement of the timber transoms that reside in the railway system. Composite steel and precast reinforced concrete transoms have been proposed as the replacement for the current timber counterparts. This paper outlines the structural benefits of composite steel-concrete transoms for ballastless tracks when retrofitted to existing railway steel bridges. However, in existing studies, it is found that there is little investigation into the effect of derailment loading on reinforced concrete transoms. Therefore, this paper provides an investigation of derailment impact loading on precast reinforced concrete transoms. The paper herein investigates the derailment impact loading of a train through experimental testing and numerical analysis of conventional reinforced concrete transoms. The paper also evaluates the potential use of 3 different shear connectors; welded shear studs, Lindapter bolts and Ajax bolts. The results of the experimental tests and finite element models are used to determine whether each transom is a viable option for the replacement of the current timber transoms on the existing bridges in Australia and whether they provide a stronger and longer lasting solution to the current transom problem.

Keywords: *Railway bridges; composite steel- concrete; retrofitting.*

1. Introduction

Transoms are one of the most important components of a railway system. They are designed as load carrying elements of a railway bridge which span under the roadway and transfer the railway loads to the trusses and beams. Current timber transoms are the most commonly used however they are susceptible to biological and chemical degradation. This reduces their service life and requires frequent maintenance and replacement. In order to fulfill the current promotion of more sustainable material, alternative materials such as composite steel-concrete panels are starting to be implemented more. The reason being that composite steel-concrete provide a material which utilises the best attributes of each individual element providing higher strength, long service life and flexibility in design.

Existing research predominantly investigates the static and dynamic loading on railway bridge structures but are limited to derailment loading onto bridge structure itself and does not consider derailment impact loading scenarios for the transoms. A case study conducted by Darwish [1] conducted a site investigation of a railway bridge in Baghdad. This research applied actual static live loading and dynamic loads to the bridge by passing a heavy locomotive over it at different speeds and stopping it in selective spots to understand how the structure reacts and deflects to different loading scenarios. Similar studies conducted by Griffin et al. [2,3] showed static tests on composite slabs, however, the studies did not investigate the derailment impact loading due to the locomotive.

To create a more consistent railway track in terms of quality and comfort for the passengers, and to provide the long-term functionality required, an alternative material must be found. In the modern era, railway locomotive speeds have been increasing as detailed by González-Nicieza et al. [4] where it is stated that improvements in transom design are mainly focused upon increasing the durability of the sleeper around the loading produced by higher speeds of the locomotive. Hence, the purpose of this paper is to fill the knowledge gap of ballastless tracks under derailment loading scenarios in the plastic region. This paper also aims to determine the failure modes and strength of conventionally reinforced composite steel-concrete transoms in order to provide a guide for engineers to use in designing railway bridges.

2. Experimental Studies

Three conventionally reinforced specimens of 2100 mm length were tested. The cross-sectional area of the transoms is 600 mm wide x 180 mm thick. The reinforcement consists of N10 stirrups at 90 mm spacing, 2 N12 and 4 N28 reinforcing bars. Figures 1 and 2 show the cross section and longitudinal section detailing of the specimens respectively. The types of connectors in the beams include 19 mm welded shear studs, 20 mm Ajax bolts and 29 mm Lindapter bolts as displayed respectively from left to right in Figure 3.

Figure 4 shows the location of the frame resisting the impact load and the location of the impact load on a longitudinal section view. The transom is set up underneath the impact loading machine, lined up with the drop hammer and bolted into place using a frame shown in Figure 4.

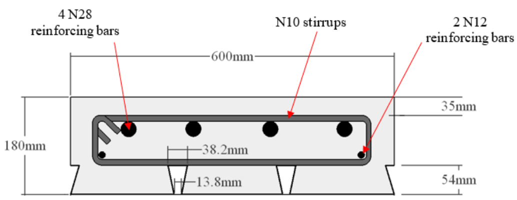

Fig. 1. Cross section dimensions

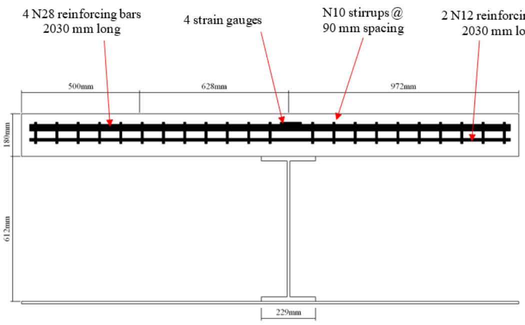

Fig. 2. Longitudinal section dimensions

Fig. 3. Shear studs utilised

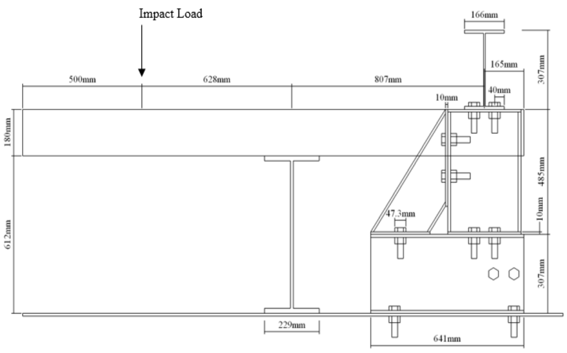

Fig. 4. Frame and impact loading locations

3. Finite Element Model

3.1. Material Properties

Through experimental analysis on the concrete presented in this research, Table 1 outlines the basic material properties.

Table 1. Elastic behaviour of concrete

Property	Value
Compressive strength, f'_c	57 MPa
Young's Modulus, E_c	34652 MPa
Poisson's ratio, v	0.2
Strain concrete, ε_c	0.003
Density, ρ	2400 kg/m^3

Regarding the plastic behaviour of the concrete, there is limited research that investigates the type of procedure that should be adopted for explicit analysis of finite element modelling. However, two common techniques are the Drucker-Prager yield criterion and the Cap Plasticity model. Both techniques are applicable for use in the FEM software Abaqus where variables regarding the internal angle of friction, cohesion of the concrete and hardening of the cap are to be defined. The two methods are similar in nature being pressure-dependent and both incorporate the hardening of the material under high strain rates. Due to this high strain rate, the cap plasticity model will be incorporated into the modelling of the concrete. The use of this material modelling procedure is used in an investigation conducted by Remennikov and Tahmeasebinia [5] where a similar loading scenario is used to produce the failure behaviour within a concrete slab. The properties are defined accordingly as presented in Table 2.

Table 2. Cap plasticity concrete material

Cohesion (MPa)	Internal angle of friction (β)	Cap eccentricity parameter (R)	Initial cap yield surface position	Ratio of flow stress (K)
4.70567	51°	0.65	1.1 x 10^{-3}	1

The initial material properties for the steel elements within the Abaqus model are presented in Table 3 where the ratios for determining ultimate stress (σ_{us}), plastic strain (ε_{ps}), and ultimate strain (ε_{us}) are summarised by Griffin [6]. The elastic modulus, E for all steel was takn as 200 GPa. There is low yield capacity in the support beam with a yield strength of 300 MPa as displayed in Table 3. This is because the steel beam that is currently used on the Sydney Harbour Bridge was designed in the 1930s. Therefore, the same capacity must also be used in this analysis to accurately simulate the behaviour of the transom.

Table 3. Steel material properties

Element	Yield Stress (MPa)	σ_{us} (MPa)	ε_{ps}	ε_{us}
Support Beam	300	1.28 σ_{ys}	10 ε_{ys}	30 ε_{ys}
Stiffener	300	1.28 σ_{ys}	10 ε_{ys}	30 ε_{ys}
Reinforcing Steel	500	1.28 σ_{ys}	9 ε_{ys}	40 ε_{ys}
Prestressing Steel	500	1.28 σ_{ys}	9 ε_{ys}	40 ε_{ys}
Bondek II	550	N/A	20 ε_{ys}	N/A
Shear Studs	420	N/A	25 ε_{ys}	N/A

For explicit analysis, the density of each material is also required to be defined so the finite element software can accurately calculate the propagation of the stress wave through the structure. The density of all steel elements was taken as 7850 kg/m^3.

3.2. Element type, mesh and contact interactions

The elements used for the nodes in this investigation are the C3D8R element. As stated by Mirza [7], this is derived from the five aspects of their behaviour; the family, degrees of freedom, number of nodes, formulation and integration. The C3D8R element is used for all parts except for the conventional reinforcement where the truss element, T3D2 is used.

Meshing is a crucial aspect of the finite element model. Due to the nature of the loading, the model is run under explicit analysis. Hence, the simulation time is directly proportionate to the smallest element length within the model. The increment size is calculated based upon the length of time taken for a wave propagating at the speed of sound to travel across the smallest length. Therefore, to reduce computation times, mesh sizing was kept large.

The importance of contact interaction is greatly increased when the composite structure is considered since the load-bearing capacity of the structure is dependent upon the interaction between one or more elements. Again, to reduce simulation times, tie constraints were used for all surfaces except for the contact between the impactor and the concrete.

3.2. Loading conditions

To compare the results obtained in this numerical analysis with the experimental analysis conducted, the target height above the transom was required to be 2 metres. Initially the impactor was displaced to the 2 metre target height and relied upon the gravity loading as defined previously to produce the velocity required for the impact. However, this caused an unnecessary and significant increase in simulation times. Therefore, the impactor was placed 200 mm above the surface of the transom and subjected to the velocity produced from a 2 metre drop using a predefined field, calculated to be 6.264 m/s.

4. Results and Discussion

4.1. Conventionally reinforced transom with AJAX bolts (CRA)

To analyse the behaviour of the concrete, there are three main points during the impact that should be outlined and discussed. These are represented by Points A, B and C in Figure 5 where the peak deflection during loading, initial permanent deformation after the initial contact and the final permanent deformation is highlighted by these points respectively. Point A displays the displacement of the impact zone for the corresponding the maximum peak load the panel can withstand and is estimated to be 28 mm. Comparatively, the peak displacement produced by the experimental data is 42 mm, corresponding to a difference of 14 mm. However, since this displacement is large when compared to the remaining data for the finite element model and occurs for a small amount of time, this result can be considered negligible.

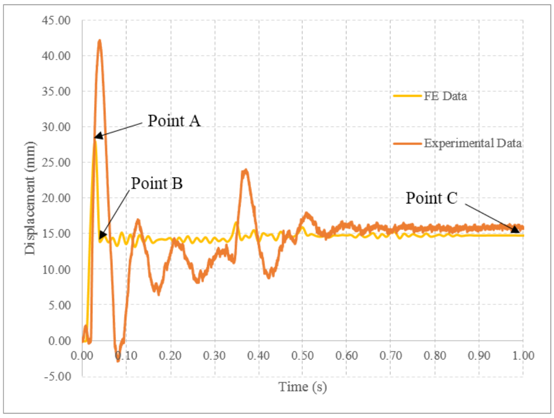

Fig. 5. Deflection behavior for CRA

After the first contact, the impactor is separated from the concrete and the transom shows signs of permanent deformation as the concrete returns to a displacement of 14 mm outlined by Point B. This corresponds to a displacement of 17 mm for the experimental data at the same point in loading and a discrepancy of 3 mm, corresponding to a 21% discrepancy due to the large vibration experienced by the beam after the initial impact. The permanent deformation at Point C in the simulation is shown to be 15 mm. The experimental data displays a similar permanent deformation of 16 mm, corresponding to a discrepancy of 1 mm and 7% increase in deflection.

Figures 6 and 7 display the cracking on the top of the experimental specimen and FE model respectively through means of stress contour plotting. Regions (1) and (2) outline the cracking through the connection that occurs in both the specimen and model where the stress has reached 10 MPa. The region highlighted here is also subjected to large amounts of bending and hence, excessive cracking that occured. Region (3) displays the stress occurring around the impact zone. Similarly with the previous regions, excessive cracking propagates from this area due to the large strain produced on the surface of the concrete during the impact loading.

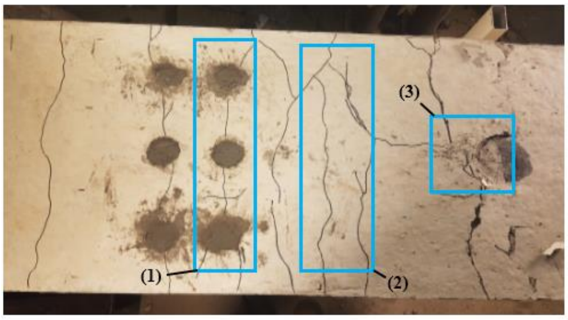

Fig. 6. Cracking behavior for Experimental CRA

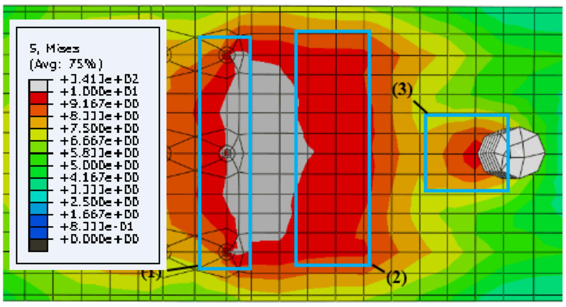

Fig. 7. Stress distribution for CRA

4.2. Conventionally reinforced transom with welded shear studs (CRW)

Point A in Figure 8 is 31 mm as a result from the first contact between the impactor and the concrete. The peak displacement produced is 47 mm. Following the initial impact, the concrete returns to a displacement of 19 mm shown in Point B. This corresponds to a displacement of 16 mm for the experimental data at the same point in loading and a discrepancy of 3 mm, corresponding to an 18% discrepancy between the two sets of data. The final permanent deformation at Point C in the simulation is shown to be 18 mm. The experimental data displays a similar permanent deformation of approximately 14 mm when averaged, corresponding to a discrepancy of 4 mm and 24% decrease in deflection. During experimental testing, the specimen was first subjected to an impact loading at a 1 metre height since it was the first specimen to be tested and was treated as a trial. However, the specimen was damaged prior to the 2 metre impact test and this significantly influences the response of the concrete to the next impact, hence, large discrepancies between the results for numerical and experimental analysis are produced.

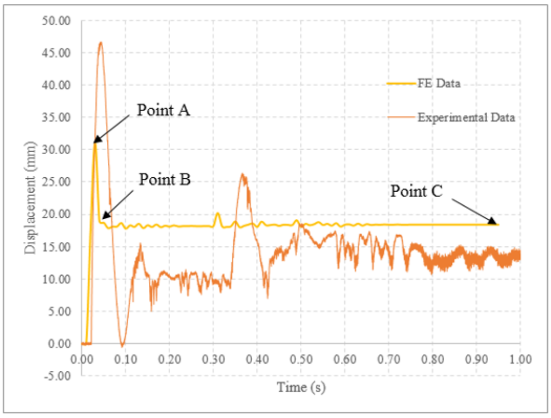

Fig. 8. Deflection behavior for CRW

Region (1) in Figures 9 and 10 outline the cracking through the connection that occurs in both the specimen and model where the stress has reached 10 MPa. The region highlighted here is also subjected to large amounts of bending and hence, excessive cracking occurs. Region (2) displays the stress occurring around the impact zone. Similarly, with the previous regions, excessive cracking propagates from this area due to the large strain produced on the surface of the concrete during the impact loading.

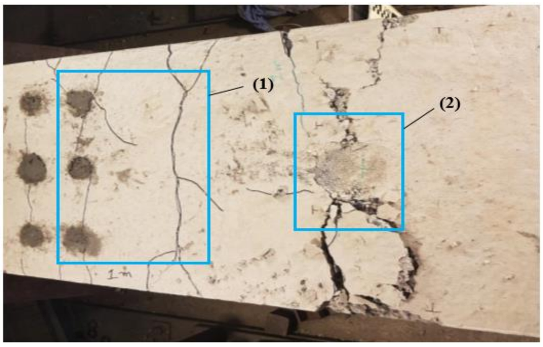

Fig. 9. Cracking behavior for Experimental CRW

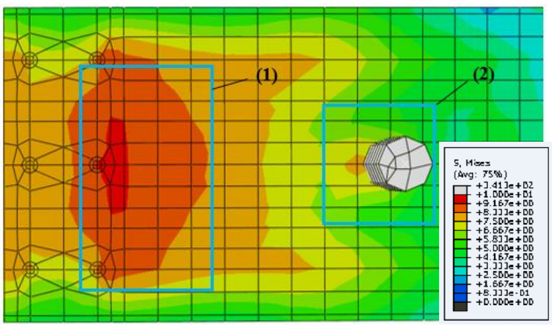

Fig. 10. Stress distribution for CRW

4.3. Conventionally reinforced transom with Lindapter bolts (CRL)

Point A in Figure 11 is 29 mm as a result from the first contact between the impactor and the concrete. Comparatively, the peak displacement produced by the experimental data is 37 mm, corresponding to a difference of 8 mm. After the first contact, the transom shows signs of permanent deformation as the concrete returns to a displacement of 10 mm outlined by Point B. This corresponds to a displacement of 13 mm for the experimental data at the same point in loading and a discrepancy of 4 mm, corresponding to a 42% discrepancy between the two sets of data. The final permanent deformation at Point C in the simulation is shown to be 12 mm. The experimental data displays a similar permanent deformation of approximately 11 mm when averaged, corresponding to a discrepancy of 1 mm and 5% decrease in deflection.

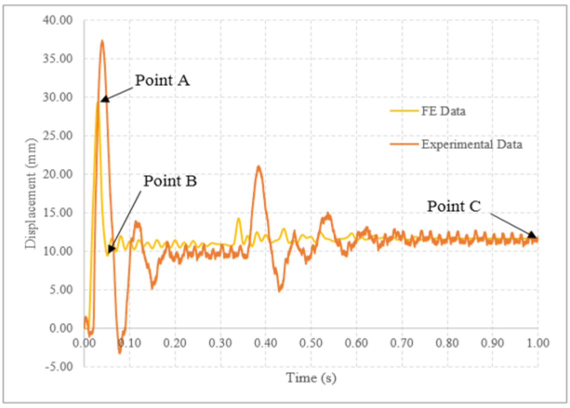

Fig. 11. Deflection behavior for CRL

Region (1) in Figures 12 and 13 outline the cracking through the connection that occurs in both the specimen and model where the stress has reached 10 MPa. The region highlighted here is also subjected to large amounts of bending and hence, excessive cracking occured. Due to the stiffness added by the shear studs, bending also happens in the area outlined by Region (2) and cracking occurs in both the numerical and experimental results. Lastly, Region (3) displays the stress occurring around the impact zone. Similarly, with the previous regions, excessive crackig propagates from this area due to the large strain produced on the surface of the concrete during the impact loading.

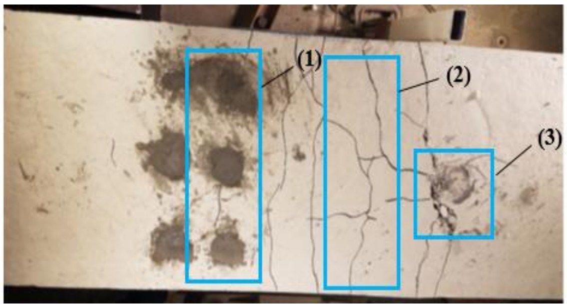

Fig. 12. Cracking behavior for Experimental CRL

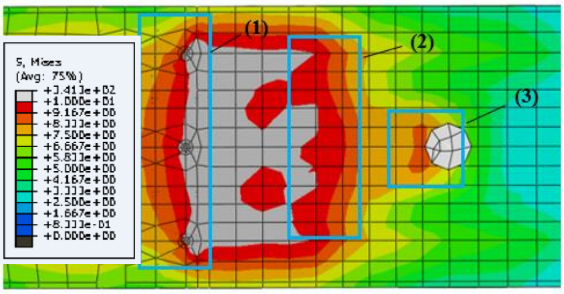

Fig. 13. Stress distribution for CRL

5. Conclusions

Three transoms were experimentally tested and modelled to determine the detailed failure behaviour of the transom and the feasibility in replacing the current timber transoms that reside on the existing steel railway bridge network. The transoms were varied using three different types of shear connectors: AJAX bolts, welded headed shear studs and Lindapter bolts to analyse the change in strength given by these shear connectors. The following conclusions were obtained from the research presented herein:

- No signs of significant failure within the concrete transom or existing steel structure were observed for either the experimental or numerical analysis. Initial and severe cracking was produced particularly around the connection due to the bending moment produced upon impact. However, the capacities of the reinforced concrete transoms exceeded the intended design load and has resulted in an overly conservative design.
- The type of shear connector was observed to have a significant effect within the conventionally reinforced transoms. Similar trends in deformation were displayed in all connectors. However, the Lindapter bolt influenced the most in strength capacities within the concrete due to the extra surface area bonding to the concrete and larger diameter, providing more stiffness to the concrete.
- Discrepancies between the numerical and experimental were minimal, promoting the validity and future use of these finite element models for parametric studies and investigations into further detail of the failure behaviour.

Acknowledgements

The authors would like to thanks Mr. Zac White from Western Sydney University and the University of Wollongong’s technical staff for their help during the testing stage. We would also like to thank the industry partners Transport for New South Wales for sharing their technical knowledge and EJF Engineering for manufacturing the frame.

References

[1] Darwish AM. Static and dynamic loading test of a railway bridge. Acta Technica Corviniensis - Bulletin of Engineering 2015; 8(2): 145-148.

[2] Griffin D, Mirza O, Kwok K, Kaewunruen S. Composite slabs for railway construction and maintenance: a mechanistic review. The IES Journal Part A: Civil & Structural Engineering 2014; 7(4): 243-262.

[3] Griffin D, Mirza O, Kwok K, Kaewunruen S. Finite element modelling of modular precast composites for railway track support structure: A battle to save Sydney Harbour Bridge. Australian Journal of Structural Engineering 2015; 16(2): 150-168.

[4] González-Nicieza C, Álvarez-Fernández MI, Menéndez-Díaz A, Álvarez-Vigil AE, Ariznavarreta-Fernández F. Failure analysis of concrete sleepers in heavy haul railway tracks. Engineering Failure Analysis 2008; 15(1-2): 90-117.

[5] Remennikov A, Tahmeasebinia F. Simulation of the Reinforced Concrete Slabs under Impact Loading. Australasian Structural Engineering Conference (ASEC), June 26-27, 2008.

[6] Griffin D. Design of Precast Composite Steel-Concrete Panels for Track Support: For Use on the Sydney Harbour Bridge. School of Civil Engineering, University of Western Sydney, Kingswood, Australia.

[7] Mirza, O. Behaviour and design of headed stud shear connectors in composite steel-concrete beams. University of Western Sydney, Australia.